Bulletin of the Seismological Society of America, Vol. 93, No. 6, pp. 2752–2757, December 2003

Short Notes

A Comparison of Synthetic Seismograms for 2D Structures: Semianalytical versus Numerical

by Sidao Ni, Vernon F. Cormier, and Don V. Helmberger

Abstract Teleseismic wave fields occasionally exhibit rapid changes in travel times and waveforms over distances less than several great-circle degrees when observed at broadband arrays. These rapid changes in wave field suggest the existence of significant structural transitions occurring over scales of several hundred kilometers or less in the mid- and deep mantle. Although approximate analytical methods based on raytracing can be readily adapted to structures having arbitrarily small scale lengths, it is important to validate their accuracy against the predictions of numerical methods. Here we compare synthetics from an approximate ray-based method WKBJ modified (WKM) against the pseudospectral method for a 2D model of the *S*-velocity anomaly associated with the South African plume. This model consists of a uniform 3% decrease in *S* velocity over a broad (>10°) region of the mid- and deep mantle beneath South Africa, contiguous at its bottom with a thin (100- to 200-km-thick) zone of low velocity extending 30° westward toward South America along the core–mantle boundary. Transitions between anomalous and radially symmetric structures of the test model are sharp, occurring over l0 km or less. *SV* and *SH* wave fields synthesized by the WKM and pseudospectral methods in this model generally agree with each other well. Slight mismatches in the two methods can be understood as the result of either differences in model parameterization or the effects of asymptotic approximations in the ray-based WKM method.

Introduction

Recent studies of the lower mantle have emphasized the prominence of anomalous high- and low-velocity regions and their association with surface tectonics. For example, the Circum-Pacific ring contains slabs near the surface and displays relatively high velocities in the lower mantle (Ritsema *et al.*, 1999). These regions typically produce visible *Scd* phases (Lay and Helmberger, 1983), having considerable variation in waveforms over short intervals of range (Sidorin *et al.*, 1998). Most of the evidence for anisotropic structures in D'' comes from these regions (Garnero and Lay, 1997). Prominent slow-velocity regions occur beneath the mid-Pacific and South Africa with some ultra-low-velocity zones (ULVZs) occurring in isolated spots, typically at the edges or transitions from fast to slow regions (Ni and Helmberger, 2001). Observations from broadband arrays indicate that some of these boundaries are quite sharp, producing multipathing visible in the short-period band (Luo *et al.*, 2001; Ni *et al.*, 2002) . Essentially, the two paths associated with the fast and slow regions become separated enough to form two discrete pulses. An example of one of these structures is displayed in Figure 1, along with ray paths for *S, ScS*, and *SKS*. To explain the differential travel times *ScS–S* and *SKS–S* for various events along this 2D section requires considerable revision of existing tomographic models. Specifically, the intensity of estimated anomalies must be doubled. Our preferred model contains a uniform 3% drop in shear velocity inside the boundary. Numerous record sections of *SKS* observed at the South African Array display rapid jumps in *SKS* travel times of up to 8 sec and complex waveforms when their associated ray paths cross these boundaries (Ni *et al.*, 2002; Ni and Helmberger, 2003b). To satisfy rapid transitions in differential travel times and waveform complexity, the edges of the low-velocity region must also be sharpened to have transitions no wider than 100 km. Evidence also exists of significant 3D, rather than 2D, structure along existing profiles, which is currently difficult to assess without denser arrays.

Fortunately, faster computers, coupled with advances in numerical methods, now allow seismograms to be synthesized in arbitrarily complex 2D and 3D structures (e.g., Komatitsch and Villote, 1998; Komatitsch and Tromp, 1999). The current generation of processors limits the practical ap-

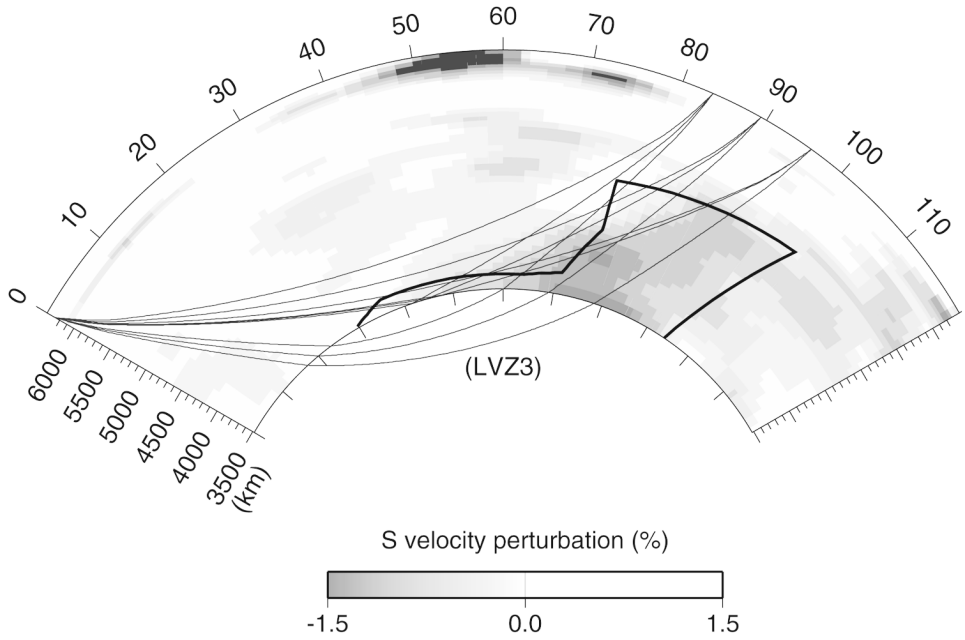

Figure 1. 2D velocity section from South America to South Africa obtained from tomography (Ritsema *et al.*, 1999). Superimposed is an enhanced structure denoted by a heavy line, which contains a uniform 3% reduction in shear velocity. Ray paths for *S, ScS*, and *SKS* are included at ranges from 85° to 95°, showing the sampling of slow structure. (After Ni and Helmberger, 2002.)

plication of numerical methods in three dimensions to relatively long periods. Most 2D problems, however, are now numerically practical in models of size 1000 × 1000 wavelengths with 10 or fewer processors in 1 day of computation. The peak frequency and maximum range in the examples shown in this article (0.2 Hz and 120°, respectively) correspond to 2000–4000 wavelengths. As of this date, approximate analytic methods for synthesizing seismograms in laterally varying structures still offer considerable computational advantages over numerical methods. Seismograms for the structure discussed in this article, for example, can be synthesized by the WKBJ modified (WKM) method in less than an hour on a single processor, making it possible to quickly explore the trade-offs in possible structures to explain observed record sections. Errors due to the effects of model parameterization in the WKM method, including extensions to geometric ray theory to model headwaves and diffractions in laterally varying structures, however, are unknown and need to be assessed. Likewise, errors associated with grid density and spacing in numerical methods also need to be assessed in new structures. It is well known, for example, that numerical methods can usually achieve high accuracy in arbitrarily complex models, but this high accuracy may sometimes require either considerable densification or warping of the grid to follow the topography of sharp boundaries and transitions (e.g., Fornberg, 1996). We will compare approximate analytic with numeric seismograms synthesized for the model displayed in Figure 1. The aims of this exercise are to check and validate the approximations of the 2D WKM method and the gridding scheme used in a 2D pseudospectral method for routine refinement of laterally heterogeneous models of the mid- and deep mantle.

Methods

WKM

Many of the commonly used methods for synthesizing seismograms were discussed in Chapman and Orcutt (1985). Their study compared numerous seismograms synthesized by the WKBJ method with those synthesized by the reflectivity method, including ranges in which triplicated and diffracted phases are generated by 1D structures of the mantle and core. Since that study, considerable progress has been made in extending WKBJ-like methods to more complex problems in three dimensions. Liu and Tromp (1996), for example, introduced a uniformly valid ray method, and more recently Rumpker and Kendall (2002) developed a Maslov-based method for treating anisotropic media. These extensions to ray-based methods require smoothly varying media. Structures with abrupt edges, such as ULVZs, appear to be tractable with hybrid methods containing analytical–numerical interfacing (Wen and Helmberger, 1998). A drawback to the hybrid approach is the considerable effort in smoothing and interfacing grids, which must be customized and tested for each specific structure. An advantage of the WKM method used here is that a relatively automatic and systematic parameterization can be applied to existing to-

mographic-type models (Ni *et al.*, 2000). The original theory in one dimension is based on Chapman (1976), which derives an approximate solution for a layered model containing ray parameters, p_i, and travel times, t_i, reflecting off each interface. The wave field can be approximated by the numerical derivative of

$$\sum_i \frac{p_i - p_{i-1}}{t_i - t_{i-1}} .$$

A similar approximation was introduced by Wiggins and Madrid (1974) based on numerical comparisons with generalized ray theory results. The procedure is displayed in Figure 2, where the first step is to generate the ray paths for a 1D reference model, as in tomography. Here we display the case of an *SKS* phase at 103°, with solid line segments indicating the paths. The boxes with the tomographic changes now take on the new velocities. We repeat the search for rays satisfying Snell's law displayed as dashed lines. Note that they become shorter by moving toward the right, with the extra paths accommodated on the faster velocities on the left side (not shown). The process could be repeated for higher resolution, but typically the correction is small (Ni *et al.*, 2000). The travel-time difference between paths bracketing the boundary has distinctly different travel times and, thus, a jump in the ($p - t$) curve (Fig. 3). These curves look like the results of WKBJ rays that sample the structure in the vicinity of the receiver but are obviously different paths (modified). This similarity in methodology is the reason for calling our procedure the "WKM method", which is short for "WKBJ modified." The density of (p_i, t_i) points is easily controlled by changing the layer thickness. The primary reason for adopting this method is ray path stability. As is well known, raytracing through 2D structures tends to produce uneven ($p - t$) curves, as discussed in Helmberger *et al.* (1985a,b), requiring careful examination of every response to identify truncation phases, and so on. Another advantage is that these (p_i, t_i) can be directly used in the Cagniard–deHoop formalism. A disadvantage is the need to compute the (p_i, t_i) ray paths at every receiver relative to WKBJ, which requires only one initial table of values (Chapman, 1976).

The ($p - t$) curves for PREM in Figure 3 are smooth and produce simple *SKS* pulses when generating the numerical ($\delta p/\delta t$), while the curves on the right contain two arrivals near the ray path crossover depending on frequency. This case of multipathing is quite simple and is likely to be very complicated for 3D structures. To produce two discrete arrivals, however, requires a sizable bundle of ray parameters with a substantial difference in travel times.

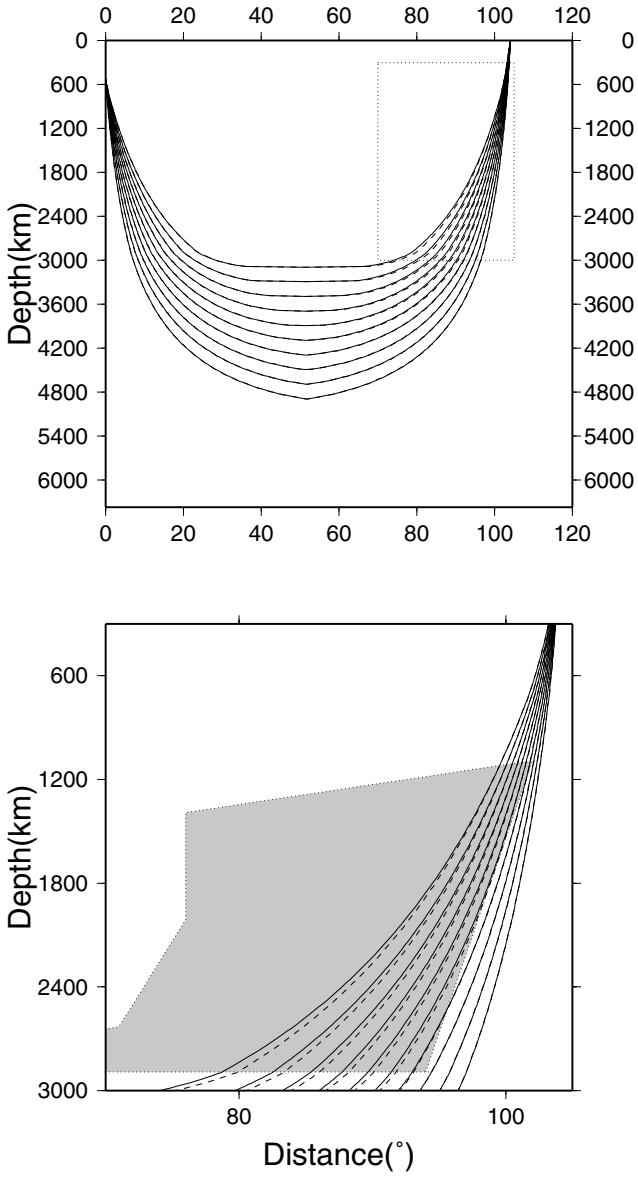

Figure 2. Display of ray paths connecting the source to the receiver after reflecting from the various interfaces satisfying Snell's law. WKM deals only with rays reflecting from each layer interface as in the Cagniard–de Hoop method (Aki and Richards, 2002). The solid lines are ray segments appropriate for the reference model, and the dashed lines indicate the perturbations after adding the velocity changes in the various blocks. The gray region indicates the slow structure, which the rays try to avoid.

Pseudospectral

The 2D pseudospectral approach used here was implemented on a multiprocessor system, as described in Cormier (2000). A velocity–stress formulation (Virieux, 1986) was applied on a 2048 × 1024 staggered grid for 32,768 time samples with a radial sampling $\delta r = 6$ km, an angular sampling $\delta = 0.0016$ (radian), and a time sampling $\delta t = 0.05$ sec. To obtain record sections having large *SKS* phases, the radial component of motion is synthesized for a vector point force applied in the radial direction. The point force has a Gaussian time history with a half-width of 1.2 sec and is located at 500-km depth and 610 km from the left side of

the grid. Periodic and antiperiodic wave fields are summed to avoid absorbing boundary conditions on the left and right sides of the grid (Furumura and Takenaka, 1995). A line-to-point source correction (Witte, 1985) and a low-pass filter cut at 0.2 Hz are applied to the calculated wave field. Intrinsic anelasticity in pure shear is included by summing three relaxations (e.g., Robertsson *et al.*, 1994; Blanch *et al.*, 1995) to approximate a frequency-independent Q equal to that of PREM in the passband low-pass filter. To include the combined effects of the assumed source time function, attenuation model, and low-pass filter assumed in the pseudospectral calculation, the 2D ray-approximate method convolved the calculated pseudospectral *SH* wave predicted observed at 90° with the wave field predicted for an assumed delta-function-shaped displacement response in the far field.

Comparisons

SV

Figure 4 compares seismograms for the radial component synthesized by the WKM method using the ($p - t$) curves shown in Figure 3 with those synthesized by the 2D pseudospectral method. Note the crossover of *S* to *SKS* is near 83°. These synthetics include the Ritsema tomographic structure (Ritsema *et al.*, 1999). To avoid the denser gridding needed to have at least four spatial samples per wavelength in the low-velocity crust, the mantle velocity and density profiles are continued to the surface in the pseudospectral synthetics. Compared to the WKM synthetics, the absence of a crust in the pseudospectral synthetics shifts arrival times earlier. The slow *SKS* arrivals are apparent between 86° and about 106°. Both sets of synthetics show broadening near 104° as the multipathing develops, although with some differences. Comparisons of WKM synthetics at shorter period with observations were given in Ni *et al.* (2002) and Ni and Helmberger (2003a), where the multipathing is even more apparent.

SH

A comparison of *SH* synthetics generated by these same codes is displayed in Figure 5, along with filtered observations. The pseudospectral modeling parameters were identical to those used for the *SV* profile, but for a transverse vector point force observed on the transverse component of motion. The WKM synthetics were generated with a Cagniard–deHoop version of the code, which treats diffracted *S* more accurately (Ni *et al.*, 2000). Following this approach, we use the ray parameters derived for each reflecting interface p_i and define the travel time t_i as

$$t_i = p_i r + h_j \left(\frac{1}{\beta_j^2} - p_i^2 \right)^{1/2},$$

where r is the horizontal distance between the source and receiver and β_j is the velocity of each segment with thickness

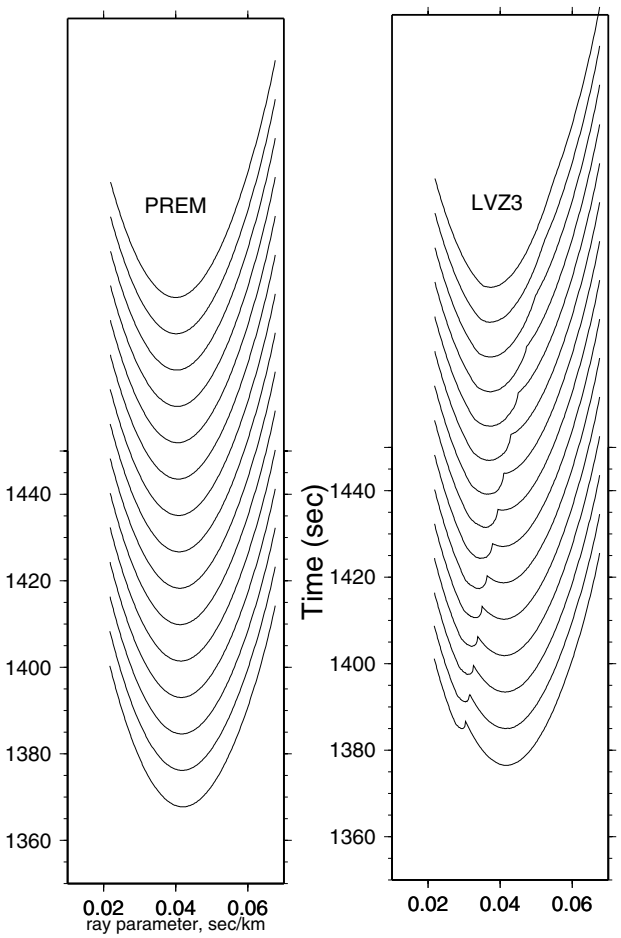

Figure 3. Construction of the ($p - t$) curves for the two models, PREM on the left. The various curves correspond to the distances 106° (top) to 104° (bottom). The two local minimums forming near the mid ranges produce two discrete pulses at short-periods, commonly referred to as "multipathing" in optics.

h_j, where we sum over the j segments. Thus, a relationship between t_i and complex p_i can be constructed and each generalized ray containing the product of all the transmission and reflection coefficient included. Models containing 2D structures can be locally stretched (Helmberger *et al.*, 1996) and accurate results produced compared against numerical codes, as displayed in Figure 5.

Discussion

Note in the comparisons shown in Figure 5 that the second pulse, which becomes a separate arrival at shorter periods (Ni and Helmberger, 2002), is a strongly delayed *ScS*. There are significant differences between these synthetics, some of which are understood. For example, the solid traces have a slightly downward trend in Figure 5 caused by its asymptotic nature, which is discussed at length in Helmberger (1973) and Chapman (1976). It becomes less of a prob-

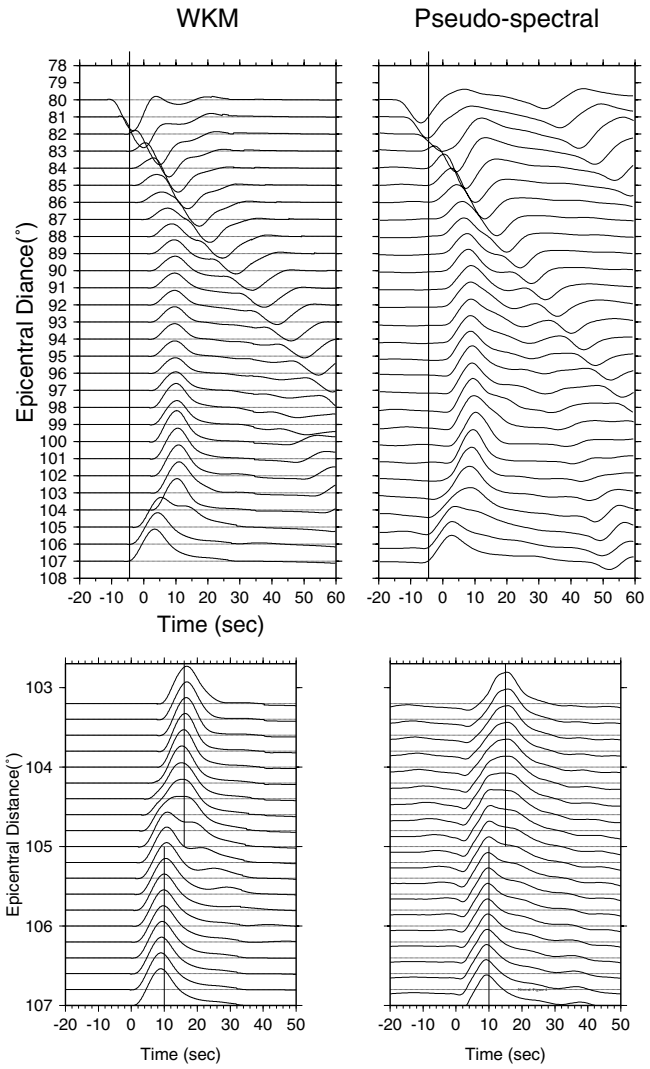

Figure 4. Comparison of *SV* synthetics generated by the WKM method (using curves as in Fig. 3) against the pseudospectral method (on the right). Note the broadness of *SKS* near the crossover from slow to fast. Enlarged images are displayed in the bottom panel. The heavy line in the upper figure indicates the predicted PREM *SKS* times. The light lines in the lower panel were added to indicate the step-over in timing.

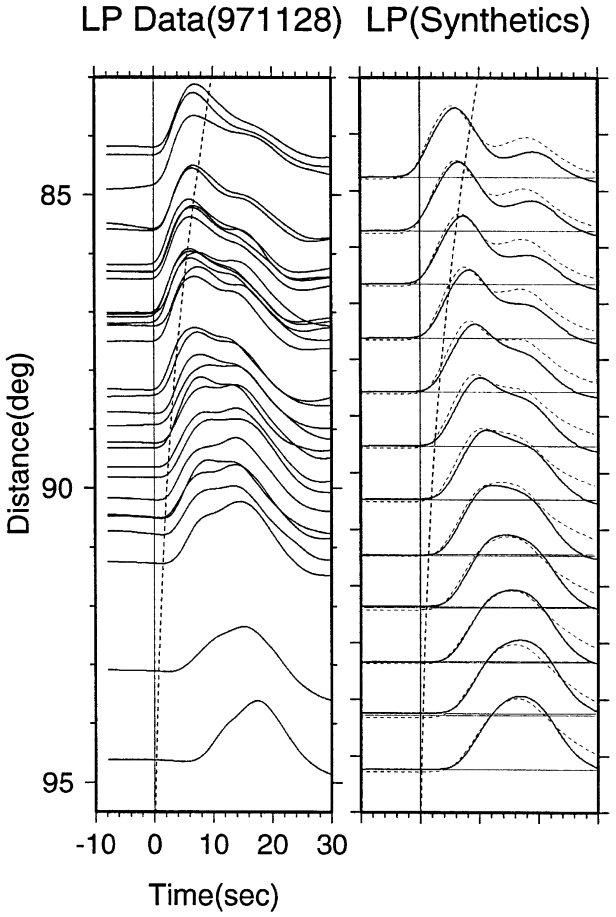

Figure 5. A profile of filtered *SH* observations (event 971128) taken from the South African Array is shown on the left; see Ni and Helmberger (2002). A comparison of *SH* synthetics is displayed on the right. The dashed curves are predictions from the pseudospectral method, and the solid curve corresponds to the analytical results, WKM + Cagniard–deHoop. The two lines correspond to PREM predictions: solid for *S* and dashed for *ScS*. Note that *ScS* is delayed over 10 sec for many records.

lem at shorter periods where this particular structure (African superplume) is being studied.

In general, the synthetics match each other well. Note that some of the observations have a second peak of slightly higher amplitude than the first, indicative of a weaker *S*- to *ScS* ratio. Although these observations are at similar distances, they are, in fact, different in azimuth, with stronger *ScS* toward the north; this is also understood by the trend of the 2D structure, which is being sampled directly by this large array (Ni and Helmberger, 2003a,b). The observations displayed here are taken at roughly right angles to the ridgelike structure, which runs for at least 7000 km into the southern Indian Ocean. Delays in diffracted *S* reach nearly 20 sec along the structure, as reported on by Wen (2001), and show evidence of 3D effects. To model such strong features will require further development of our simulating tools, but the two methods discussed here show considerable promise. We can conclude that for at least these levels of velocity perturbation and sharpness of anomaly transitions, both the 2D WKM and 2D pseudospectral techniques and their associated parameterizations and gridding are sufficiently accurate to safely allow structural interpretation of observed profiles.

Acknowledgments

This research was supported by the NSF under Grant Number EAR-0229885. This is contribution number 8949, Division of Geological and

Planetary Sciences, California Institute of Technology, Pasadena, California. We are also grateful that Diane Doser, the associate editor, and an anonymous reviewer provided helpful comments on improving the manuscript.

References

Aki, K., and P. G. Richards (2002). *Quantitative Seismology*, Second Ed., University Science Books, Sausalito, California.

Blanch, J. O., J. O. A. Robertsson, and W. W. Symes (1995). Optimally efficient constant-*Q* modeling, *Geophys.* **60,** 176–184.

Chapman, C. H. (1976). Exact and approximate ray theory in vertically inhomogeneous media, *Geophys. J. R. Astr. Soc.* **46,** 201–233.

Chapman, C. H., and J. A. Orcutt (1985). The computation of body wave synthetic seismograms in laterally homogeneous media, *Rev. Geophys.* **23,** 105–163.

Cormier, V. F. (2000). *D″* as a transition in the heterogeneity spectrum of the lowermost mantle, *J. Geophys. Res.* **105,** 16,193–16,205.

Fornberg, B. (1996). *A Practical Guide to Pseudospectral Methods*, Cambridge U Press, New York.

Furumura, T., and H. Takenaka (1995). A wraparound elimination technique for the pseudospectral wave synthesis using an antiperiodic extension of the wavefield, *Geophys.* **60,** 302–307.

Garnero, E., and T. Lay (1997). Lateral variations in lowermost mantle shear wave anisotropy beneath the North Pacific and Alaska, *J. Geophys. Res.* **102,** 8121–8135.

Helmberger, D. V. (1973). Numerical seismograms of long-period body waves from seventeen to forty degrees, *Bull. Seism. Soc. Am.* **63,** 633–646.

Helmberger, D. V., G. Engen, and S. Grand (1985a). Notes on wave propagation in laterally varying structure, *J. Geophys.* **58,** 82–91.

Helmberger, D. V., G. Engen, and S. Grand (1985b). Upper-mantle cross-section from California to Greenland, *J. Geophys.* **58,** 92–100.

Helmberger, D. V., L. S. Zhao, and E. J. Garnero (1996). Construction of synthetics for 2D structures, in *Seismic Modeling of Earth Structure* E. Boschi, G. Ekstrom, and A. Morelli (Editors), North-Holland, New York, 183–222.

Komatitsch, D., and J. Tromp (1999). Introduction to the spectral-element method for 3D seismic wave propagation, *Geophys. J. Int.* **139,** 806–822.

Komatitsch, D., and J. P. Villote (1998). The spectral element method: an efficient tool to simulate the seismic response of 2D and 3D geological structures, *Bull. Seism. Soc. Am.* **88,** 368–392.

Lay, T., and D. V. Helmberger (1983) A shear velocity discontinuity in the lower mantle, *Geophys. Res. Lett.* **10,** 63–66.

Liu, X., and J. Tromp (1996) Uniformly valid body-wave ray theory, *Geophys. J. Int.* **127,** 461–491.

Luo, S., S. Ni, and D. V. Helmberger (2001). Ultra low velocity zone revealed from multipathed PKPab, *Earth Planet. Sci. Lett.* **189,** 155–164.

Ni, S., and D. V. Helmberger (2001). Horizontal transition from fast (slab) to slow (plume) structures at the core–mantle boundary, *Earth Planet. Sci. Lett.* **187,** 301–310.

Ni, S., and D. V. Helmberger (2003a). Ridge-like lower mantle structure beneath South Africa, *J. Geophys. Res.* **108,** no. B2, 2094, doi: 10.1029JB001545, 2003.

Ni, S., and D. V. Helmberger (2003b). Seismological constraints on the South African superplume: could be the oldest distinct structure on Earth, *Earth Planet. Sci. Lett.* **206,** 119–131.

Ni, S., X. Ding, and D. V. Helmberger (2000). Constructing synthetics from deep earth tomographic models, *Geophys. J. Int.* **140,** 71–82.

Ni, S., E. Tan, M. Gurnis, and D. V. Helmberger (2002). Sharp sides to the African Super Plume, *Science* **296,** 1850–1852.

Ritsema, J., H. Van Heijst, and J. Woodhouse (1999). Complex shear wave velocity structure imaged beneath Africa and Iceland, *Science* **286,** 1925–1928.

Robertsson, J. O. A., J. O. Blanch, and W. W. Symes (1994). Viscoelastic finite-difference modeling, *Geophys.* **59,** 1444–1456.

Rumpker, C., and J. M. Kendall (2002). A Maslov propagator seismogram for weakly anisotropic media, *Geophys. J. Int.* (in press).

Sidorin, I., M. Gurnis, D. V. Helmberger, and X. Ding (1998). Interpreting *D″* seismic structure using synthetic waveforms computed from dynamic models, *Earth Planet. Sci. Lett.* **163,** 31–41.

Virieux, J. (1986). *P-SV* wave propagation in heterogeneous media: velocity stress finite-difference method, *Geophys.* **51,** 889–901.

Wen, L. (2001). Seismic evidence for a rapidly varying compositional anomaly at the base of the Earth's mantle beneath the Indian Ocean, *Earth Planet. Sci. Lett.* **194,** 83–95.

Wen, L., and D. V. Helmberger (1998). A 2D *P-SV* hybrid method and its application to modeling localized structures near the core-mantle boundary, *J. Geophys. Res.* **103,** 17,901–17,918.

Wiggins R. A., and J. A. Madrid (1974) Body wave amplitude calculations, *Geophys. J. R. Ast. Soc.* **37,** 423–433.

Witte, D. (1985). The pseudospectral method for simulating wave propagation, *Ph.D. Thesis*, Columbia University, New York.

Seismological Laboratory
Caltech 252-21
Pasadena, California 91125
(S.N., D.V.H.)

Department of Geology and Geophysics
University of Connecticut
354 Mansfield Road
Storrs, Connecticut 06269
(V.F.C.)

Manuscript received 6 January 2003.